

An analysis of the energetics involved in the H I supershells

L. A. Suad¹, C. F. Caiafa^{1,2}, S. Cichowolski³, and E. M. Arnal^{1,4}

¹ Instituto Argentino de Radioastronomía (CCT-La Plata, CONICET; CICPBA), C.C. No. 5, 1894, Villa Elisa, Argentina.

² Facultad de Ingeniería, Universidad de Buenos Aires (FIUBA), C.A.B.A., Argentina.

³ Instituto de Astronomía y Física del Espacio (CONICET-UBA), Ciudad Universitaria, C.A.B.A., Argentina.

⁴ Facultad de Ciencias Astronómicas y Geofísicas, Universidad Nacional de La Plata, La Plata, Argentina.

October 28, 2017

ABSTRACT

Aims.

Methods.

Results.

Key words. GS- shells κ -mechanism – stability of gas spheres

1. Introduction

The interstellar medium (ISM) presents several features like bubbles, shells, supershells, worms that modifies the structure and dynamics of the Galaxy. In particular neutral hydrogen (H I) Galactic supershells (GS) are arc-like structures, detected in a certain velocity range that could be surrounded, partially or completely, by walls of H I emission. They are detected predominantly in the H I emission distribution although they can also be detected at other wavelengths (infrared, CO, optical). These are huge structures which radius varies from 100 to 500 pc according to Suad et al. (2014).

The origin of these structures is currently a subject of debate. Given that about 70 % of the massive stars in the Galaxy belongs to clusters or OB associations, the most probable mechanism for the GS formation could be the continuous energy injection from multiple massive stars (?). Other mechanisms have been proposed to explain its origin, for example the in-fall of high velocity clouds with the Galactic plane (Tenorio-Tagle 1981). One way of differentiating which mechanism took place, it is to know its kinetic energy. To this end, it is necessary to know the mass of the structures.

Aca hay que describir un poco el catálogo (explicar que hay estructuras con 1, 2, y 3 cuadrantes llenos)

hay en el catalogo 308 con 4 cuadrantes llenos y 182 con 3 cuadrantes llenos

The goal of this paper is to have an estimation of the kinetic energy involved in the GSs from the catalog of Suad et al. (2014). To this end it is necessary to have a good estimation of the GSs masses.

In this work we have developed an algorithm that automatically detects the boundaries of supershells and calculates their associated masses. We applied the algorithm to the GSs cataloged in the paper of Suad et al. (2014).

2. Observations

H I data were retrieved from the Leiden-Argentine-Bonn (LAB) survey (Kalberla et al. 2005). This database has an angular reso-

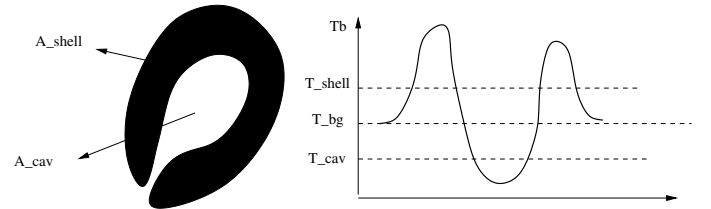


Fig. 1.

lution of $34''$, a velocity resolution of 1.3 km s^{-1} , a channel separation of 1.03 km s^{-1} , and it covers the velocity range from -400 to $+450 \text{ km s}^{-1}$. The entire database has been corrected for stray radiation (Kalberla et al. 2005).

3. Estimation of GS's masses

In this Section we describe the mechanisms used to estimate the amount of H I mass contained in the GSs.

As mentioned above, the GSs are large voids surrounded completely or partially by walls of H I emission. A sketch of a prototypical feature is shown in Fig. 1, along with a profile showing the different temperatures that characterizes each GS. Based on the hypothesis that before the structure was formed the H I was uniformly distributed, we can assume that the excess mass in the shell should be equal to the mass missing in the void. Thus, we can measure both, the excess mass of the H I shell that borders the cavity, denoted by $M_{\text{HI}}^{\text{shell}}$, and the mass missing in the void, which we will refer to as the missing mass, $M_{\text{HI}}^{\text{miss}}$. In an ideal case these two values should be exactly the same, however, owing to inhomogeneities present in the ISM where the structures are located, the estimated values do not always match.

Under the assumption that the H I gas is optically thin, the neutral masses of an H I structure located at a distance of D kpc and having an angular size Ω_{am2} arcmin² can be easily estimated by

$$M_{\text{HI}}(M_{\odot}) \approx 1.3 \times 10^{-3} D_{\text{kpc}}^2 \Delta v_{\text{km s}^{-1}} \int \Delta T_b d\Omega_{\text{am2}} \quad (1)$$

which gives an approximation to an exact integral over velocity, we just take $\Delta v_{\text{km s}^{-1}}$ as the velocity interval over which the GS is visible.

To estimate the excess mass in the shell and the missing mass in the cavity, we define three temperatures that characterizes the structure: T_{cav} and T_{shell} as the average brightness temperature in the cavity and in the shell, respectively, and T_{bg} as the background temperature (see Fig. 1). Thus, from Eq. 1 we obtain $M_{\text{HI}}^{\text{shell}}$ and $M_{\text{HI}}^{\text{miss}}$ replacing ΔT_b by $(T_{\text{shell}} - T_{\text{bg}})$ and $(T_{\text{cav}} - T_{\text{bg}})$, respectively.

3.1. Estimation by hand

To estimate the neutral masses of a given structure it is necessary to first determine all the involved parameters: the distance, the velocity interval where the structure is observed, the three temperatures defined above, and the angular size of the shell and the cavity.

As a first step, by inspecting the H I data-cube, the velocity interval where the supershell is better observed is determined and used to create a velocity averaged image. Secondly, this image is used to estimate the three temperatures and both angular areas. Clearly, all these values have a large uncertainty, which must be taken into account in the value of the mass. For instance, given the nonuniform background, the determination of the shell location is usually quite subjective and not easy. To determine T_{bg} we consider the value of the contour level defining the outer border of the H I void, which represents the temperature of the neighboring gas. This contour is also used to define the angular extent of the cavity and the inner border of the shell.

Taking into account all the errors involved, we can assume that the masses calculated using Eq. 1 have an error of not less than 50%.

3.2. Automatic algorithm

4. Validation of the algorithm

Since the goal of this paper is to determine the kinetic energy stored in all the Galactic supershell candidates having four or three filled quadrants in the recently published catalogue of Suad et al. (2014), we need first to be confident that the masses obtained by the algorithm can be trusted.

To test the values yield by the algorithm, we have measured individually the masses of 92 GS belonging to the catalogue, 60 with four filled quadrants (group A from hereon) and 32 with three filled quadrants (group B from hereon). It is important to mention that the 92 GS were randomly selected, so the sample contains structures having different shapes and located in different regions of the outer part of the Galaxy (at both high and low Galactic latitudes and near the Galactic plane).

Following the procedure described in Section 3.1 and using Eq. 1 we estimated the 92 excess and missing masses for structures of group A and B shown in Table 1 and Table 2, respectively. The distance d , and the velocity interval where the GS is visible $\Delta v_{\text{km s}^{-1}}$ adopted for each structure were taken from the catalogue (Suad et al. 2014).

Figure aa and bb show a comparison between the shell masses, $M_{\text{HI}}^{\text{shell}}$, and the missing ones, $M_{\text{HI}}^{\text{miss}}$, obtained by hand and by the algorithm, for group A and group B, respectively. As can be seen, assuming an error of 50% for all the estimations, the values obtained from both procedures agrees in a hh% (group A) and ff% (group B) of the structures.

aca va el motivo de las que no coinciden

5. Kinetic energy estimation

References

- Kalberla, P. M. W., Burton, W. B., Hartmann, D., et al. 2005, A&A, 440, 775
 Suad, L. A., Caiafa, C. F., Arnal, E. M., & Cichowolski, S. 2014, A&A, 564, A116
 Tenorio-Tagle, G. 1981, A&A, 94, 338

Acknowledgements.

Table 1. Shell and missing masses obtained for sample A.

ID	$M_{\text{HI}}^{\text{shell}} (\text{Hand})$ $\times 10^4 M_{\odot}$	$M_{\text{HI}}^{\text{miss}} (\text{Hand})$ $\times 10^4 M_{\odot}$	$M_{\text{HI}}^{\text{shell}} (\text{Alg.})$ $\times 10^4 M_{\odot}$	$M_{\text{HI}}^{\text{miss}} (\text{Alg.})$ $\times 10^4 M_{\odot}$
GS093-06-034	5.06	2.78	6.21	5.59
GS100-06-019	5.16	2.70	1.48	1.48
GS101-02-037	11.70	6.62	7.47	6.76
GS101+29-026	5.93	4.96	8.10	8.10
GS102-08-054	10.70	6.06	11.36	6.90
GS104+03-038	6.20	3.90	5.85	5.85
GS105-12-040	2.42	2.33	1.53	1.51
GS107+02-069	7.14	4.40	2.47	2.47
GS107+13-040	3.80	2.04	2.62	2.78
GS108-03-022	8.31	5.23	9.79	9.79
GS108+03-088	3.26	1.68	7.91	4.90
GS113-01-075	9.10	4.69	8.69	8.70
GS113-14-042	3.64	3.21	5.56	5.56
GS114-03-054	1.86	0.96	5.97	5.97
GS114-05-062	4.21	3.94	2.14	1.94
GS115-05-054	2.24	1.80	1.99	2.01
GS118+01-044	3.79	5.12	15.54	15.34
GS119-04-058	7.10	4.86	9.82	9.89
GS121-05-037	11.10	5.85	6.46	6.49
GS122-02-077	33.80	25.00	4.66	4.30
GS124-09-043	4.25	2.30	20.73	20.78
GS129+05-061	21.10	10.50	5.73	3.97
GS133-07-045	15.80	9.75	16.43	16.14
GS135-09-056	5.44	4.77	13.88	13.87
GS136-09-033	2.25	1.30	0.57	0.57
GS137+03-063	4.24	2.24	5.51	5.51
GS138+02-053	2.62	1.38	6.86	5.38
GS140-03-079	29.70	25.10	57.83	57.84
GS141-10-042	2.88	1.85	4.20	4.19
GS144+08-031	6.51	3.50	5.34	5.34
GS146-11-025	1.21	0.91	7.85	7.86
GS146-11-045	0.41	0.22	2.38	0.72
GS153+02-047	2.46	1.40	7.79	7.74
GS164+00-021	2.88	3.07	5.81	6.50
GS195+28+014	0.31	0.24	0.48	0.48
GS198-01+035	3.57	2.03	5.80	5.82
GS199-13+025	0.54	0.27	0.94	0.79
GS201-23+025	0.40	0.21	0.17	0.14
GS202+10+014	0.64	0.37	0.17	0.17
GS221-03+045	2.75	1.76	4.83	4.87
GS222+13+026	0.56	0.40	1.09	1.09
GS227+05+051	0.95	0.63	2.00	2.00
GS229+03+073	2.22	1.22	3.05	3.05
GS230-06+040	6.35	3.55	18.74	18.91
GS232+02+081	3.26	1.72	2.70	2.76
GS239-02+068	7.21	4.69	23.20	19.29
GS240+00+035	0.48	0.47	0.32	0.32
GS240+05+033	0.53	0.40	0.57	0.57
GS246+07+048	0.59	0.57	1.05	1.05
GS247+00+086	7.47	3.75	6.44	5.37
GS253-12+053	4.56	2.95	0.66	0.59
GS253+07+062	10.00	5.18	8.34	8.33
GS256-16+055	1.17	0.77	0.55	0.55
GS257+00+067	2.01	1.18	2.30	2.31
GS259-08+090	10.90	6.65	19.86	19.86
GS260-04+081	3.72	3.70	2.37	2.35
GS261-03+055	2.49	1.65	3.10	3.10
GS263+10+020	1.33	1.39	2.20	2.19
GS265-06+082	12.80	6.75	6.56	6.36
GS269+04+044	6.09	3.15	8.21	8.21

Table 2. Shell and missing masses obtained for sample *B*.

ID	$M_{\text{HI}}^{\text{shell}}(\text{Hand})$ $\times 10^4 \text{ M}_{\odot}$	$M_{\text{HI}}^{\text{miss}}(\text{Hand})$ $\times 10^4 \text{ M}_{\odot}$	$M_{\text{HI}}^{\text{shell}}(\text{Alg.})$ $\times 10^4 \text{ M}_{\odot}$	$M_{\text{HI}}^{\text{miss}}(\text{Alg.})$ $\times 10^4 \text{ M}_{\odot}$
GS089-21-025*	3.26	4.05	6.18	7.00
GS093-14-021*	8.88	4.50	28.37	28.14
GS093+11-034*	2.54	1.28	1.88	1.88
GS098-25-018*	1.08	1.08	1.47	1.16
GS098+24-032	0.96	0.81	2.58	2.58
GS100+09-040*	5.34	2.99	8.14	8.14
GS101-13-056*	24.00	16.90	18.69	18.68
GS105-03-061	22.40	12.40	5.34	3.93
GS108+00-075*	4.67	2.86	9.47	9.48
GS109+06-032	2.50	1.65	3.94	3.97
GS109+16-033*	6.54	7.24	6.76	6.75
GS110-04-067	7.80	7.15	5.74	2.79
GS116-06-042*	2.49	1.89	5.95	5.97
GS117+08-076*	5.49	3.92	17.51	17.62
GS120+08-028	3.20	1.97	2.19	2.15
GS120+16-067*	6.54	3.79	3.57	3.59
GS130+00-068*	1.52	0.83	0.21	0.16
GS139+06-054*	3.20	0.87	2.39	2.17
GS142-01-057	2.03	1.26	2.67	2.67
GS142-01-057	7.86	10.10	2.67	2.67
GS153-10-026*	1.55	1.55	0.42	0.42
GS153-10-026*	1.78	1.01	0.42	0.42
GS161+03-036	34.50	19.40	28.47	21.79
GS202+05+031	1.74	0.92	8.99	8.97
GS218-05+037*	0.80	0.80	3.96	3.96
GS224-18+036	0.30	0.22	1.01	1.01
GS240-13+064*	1.60	1.45	2.33	2.33
GS246-05+086	2.67	1.94	1.14	1.21
GS247+06+055*	0.88	1.12	3.07	3.08
GS252-04+074*	11.40	7.82	47.88	47.82
GS257-25+030*	0.58	0.30	0.42	0.42
GS257+09+037	4.99	2.86	5.33	5.35
GS262-09+048*	5.52	3.95	3.27	3.41
GS263-08+068*	13.70	11.90	9.99	10.00
GS264-04+044	3.90	2.23	2.42	2.42
GS103+07-018*	8.54	8.28	21.58	21.60